International Journal of Energy and Environmental Engineering (2023) 14:601–612
https://doi.org/10.1007/s40095-022-00537-x

ORIGINAL RESEARCH

Investigating the effects of nanorefrigerants in a cascaded vapor compression refrigeration cycle

Evidence Akhayere[1] · Victor Adebayo[2] · Michael Adedeji[2] · Muhammad Abid[4] · Doga Kavaz[1,3] · Mustafa Dagbasi[2]

Received: 15 May 2022 / Accepted: 9 September 2022 / Published online: 29 September 2022

Abstract

It is vital, following the Kyoto Protocol, to find environmentally benign and energy-efficient refrigerants, consequently boosting the coefficient of performance (COP). Refrigeration systems are used extensively in the industrial, home, and commercial sectors for cooling, heating, food preservation, and cryogenic purposes. Researchers have successfully employed the application of nanoparticles in cooling systems to achieve improved enhancement, reliability, and efficiency of refrigeration systems because of their higher heat transfer and thermophysical capabilities. The function of numerous variables, however, makes the experimental technique appear to be costly and time-consuming to carry out. This study was, therefore, designed to numerically simulate the performance assessment of a nanoparticle-enhanced Cascaded Vapor Compression Refrigeration Cycle (CVCRC). The focus of this paper is on four distinct SiO_2 nanoparticle nanorefrigerants and their pure fluids: two HFCs as well as two fourth-generation refrigerants (HFOs), namely; R12, R134a, R1234yf, and R-1234ze (E). The results show that adding nanoparticles to the pure refrigerant improves COP, and the highest values were achieved with the R1234ze(E)/SiO2 mixture. Increasing the mass concentration of the nanoparticles leads to an increase in the refrigeration effect, an increase in COP, and a reduction in compressor work. Although R125 had the lowest compressor work of 47.12 kW when SiO2 nanoparticles are introduced, however, is not suitable for refrigeration because of its high GWP values. R1234ze has the second-lowest compressor work of 59.58 kW with the addition of SiO_2, it is consequently more energy efficient and can be used in its place as it has a GWP of 6, among other benefits.

Keywords Nanorefrigerants · COP · Refrigeration · Cascaded vapor compression refrigeration cycle · Compressor work

List of symbols

h	Specific enthalpy (kJ/kg)
ρ	Density
Q	Heat rate (kW)
W	Work rate (kW)
m	Mass flow rate (kg/s)
ω	Mass fraction

Abbreviations

BGS	Barley grass straw
COP	Coefficient of performance
CVCRC	Cascade vapor compression refrigeration system
EDX	Energy dispersive X-ray
FTIR	Fourier-transform infrared spectroscopy
GWP	Global warming potential
HFE	Hydrofluoroethers
HTL	High temperature loop
LTL	Low temperature loop
NS	Nanosilica
SEM	Scanning electron microscopy
XRF	X-ray fluorescence
HC	Hydrocarbon
HFO	Hydrofluoro olefin

Subscripts

c	Condenser
comp	Compressor
ev	Evaporator

✉ Victor Adebayo
vadebayo@ciu.edu.tr

1 Department of Environmental Science, Cyprus International University, Nicosia, Mersin 10, Turkey

2 Department of Energy Systems, Cyprus Internatonal University, Nicosia, Mersin 10, Turkey

3 Department of Bioengineering, Cyprus International University, Nicosia, Mersin 10, Turkey

4 Department of Energy Systems Engineering, Faculty of Integrated Technologies, Universiti Brunei Darussalam, Jalan Tungku Link BE 1410, Bandar Seri Begawan, Brunei Darussalam

exp	Expansion
NR	Nanorefrigerant
PR	Pure refrigerant

Introduction

The proliferation of refrigeration and air conditioning devices has significantly boosted global energy consumption. Therefore, a small reduction in energy consumption can have a big impact on the global energy situation. This necessitates the use of energy-efficient and high-performance heating, refrigeration, and air-conditioning systems.

Vapor compression cycles are the most common technology for modifying the environment of a closed room through heating or cooling [1]. Due to the high compression requirements, a single cycle system will not be able to efficiently cool processes at extremely low temperatures. To attain the requisite low temperature, cascaded refrigeration systems (CRS) are typically employed. A cascaded cooling system is made up of two cooling cycles linked by a heat exchanger. The heat exchanger acts as a condenser in the low-temperature loop (LTL) and as an evaporator in the high-temperature loop (HTL) [2].

In comparison to a single vapor compression refrigeration system, a cascaded vapor compression refrigeration system may operate at lower evaporation temperatures and compression ratios (in each loop), while yet achieving a better volumetric compressor efficiency [3]. The development of energy-efficient cooling systems is hampered by the poor thermal transport properties of conventional heat transfer fluids. To get around this constraint, a colloid has been developed through the suspension of nanoparticles (NP) into the conventional heat transfer fluids, also referred to as nanofluids [4]. Because of their thermal transfer capabilities, nanofluids have been particularly attractive as advanced working fluids. Nanofluids are made up of extremely small particles (1–100 nm) mixed with ordinary working fluids like water and oil. It is called nanorefrigerant when a refrigerant is used as the base fluid [5].

The nanorefrigerant has a higher thermal conductivity than the base fluid as a result of its superior thermal conductivity. Their higher heat transfer coefficient is also one of their most distinctive features. [6]. As a result, at the liquid, vapor, and the two-phase region of a refrigeration cycle, an increase in heat transfer takes place [7, 8]. According to the literature, the results of such contrary effects are often combined with a COP increase of about 10–20%, depending mainly on the NP and their mass/volume fraction [9].

Conventional refrigerants significantly contribute to global warming and thereby damage the ozone layer. Therefore, the performance of the vapor compression cooling system must be enhanced using a suitable refrigerant. Water was one of the first substances to be utilized as a refrigerant [10]. These water-based refrigeration systems, however, were only used in a few applications due to their numerous drawbacks. The vapor compression refrigeration systems, which used ethyl ether as the refrigerant, were first created by Jakob Perkins [11]. Due to its high boiling point, toxicity, and flammability problems, ethyl ether first seemed to be an excellent refrigerant but did not catch on. Later, the carbon dioxide-powered vapor compression refrigeration system was invented. Due to its nonflammability and lack of hazardous properties, carbon dioxide has numerous uses, particularly in marine refrigeration [10].

The initial vertical ammonia compressor with single acting was developed by David Boyle in 1872. The thermophysical properties of ammonia are excellent, it is widely available, and it is inexpensive[12]. But, ammonia is risky and has a minor flammability issue. A few common building materials, like copper, are also incompatible with it. However, testing on several other fluids, including isobutane, ethyl chloride, methyl and ethyl amines, and methylene chloride, was stopped due to several limitations [10].

The introduction of second-generation refrigerants was necessary because virtually all first-generation refrigerants had safety issues, such as toxicity, flammability, and high operating pressures. Second-generation refrigerants, also referred to as ODS, have been connected to both significant contributions to global warming and ozone layer depletion. This prompted scientists to rethink their search for safer refrigerants. This time, the phrase "safer" refers to hazards to immediate personal safety as well as long-term environmental safety, such as toxicity and flammability [10].

Between 1990 and 2009, the Montreal Protocol drastically decreased CFC emissions. Due to the non-ozone depleting characteristics becoming the major criteria for third-generation refrigerants, two alternatives HFCs and HFEs have emerged. The Montreal Protocol's primary goal was to protect the ozone layer, but it also had the unintended consequence of significantly reducing greenhouse gas emissions. This is true since HFCs emit greenhouse gases at a lower rate than CFCs. Nevertheless, the Kyoto Protocol classifies HFCs as greenhouse gases [13, 14] because of their relatively large GWP, which is many times more than CO_2. Among all greenhouse gases, HFCs are growing at the quickest pace, at a rate of 10–15% annually. Fluorochemicals were still the main topic of attention, though. Many non-fluorochemicals and hydrofluoroether (HFE) chemicals were thoroughly assessed by corporate and public research programs, but only a small number of them showed promise [10].

Several industries have been obliged to adopt a new generation of low-GWP refrigerants, such as HC (hydrocarbon) and HFO (hydrofluoro olefin) refrigerants, to meet regulatory requirements. Due to increasing international concerns

about the GWP of HFC refrigerants. The number of fluorine atoms in HFCs directly affects their atmospheric lifetime and GWP. As a result, HFCs have been scrutinized for their role in greenhouse gas emissions. The growing concern about humanity's effect on global warming has prompted researchers to look for alternative refrigerants with a lower GWP, and natural refrigerants have re-sparked renewed interest [15].

HFOs which are also called fourth-generation refrigerants are unsaturated organic compounds made up of hydrogen, fluorine, and carbon. They have a carbon–carbon double bond, which is a key feature that contributes to their low global warming. These synthetic refrigerants, known as hydrofluoro olefins (HFOs), have a low GWP which is 0.1% of that of HFCs. The HFOs, besides having short atmospheric lifetimes, have many useful properties, including low boiling points, excellent physicochemical properties, and strong vapor pressures at room temperature. As a result, they are thought to be the best HFC alternatives [10].

In this vital phase of the transition from high-GWP to low-GWP systems, this type of study might be tremendously valuable in improving knowledge regarding the application and efficiency of environmentally friendly refrigerants. Although more research is needed to fully understand nanorefrigerants' potential applicability in refrigeration and air conditioning systems, their impact on the thermodynamic efficiency of refrigerants and lubricants suggests they will be employed more frequently in the future [16]. Nanorefrigerant studies are, however, still in the embryonic phase but scientists have recently used nanoparticles in refrigeration systems because thermophysical and heat transfer capabilities could be significantly improved by these nanoparticles. Nanofluid investigations are not limited to thermal conductivity only. Nevertheless, researchers have studied other thermophysical properties as well as viscosity, the tension on the surface, specific heat capacity, etc.

Various studies on the application of nanorefrigerants in various systems are reviewed in this paper and are provided in this section. Subramani and Prakash [17] examined the performance of an Al_2O_3 nanoparticle (size and 50 nm, density 0.26 g/cc) cooling system mixed with lubricating oil (SUNISO 3GS). The results showed that refrigerant cooling in the condenser decreases by 8.3 °C and cooling time by 27%. In addition, power consumption was reduced by 25%, and COP improvement of 33% was achieved. Jwo et al. [18] also investigated the potential of Al_2O_3 nanoparticles as R12/MO additives. The results showed that a greater compression ratio compared to R12 is achieved by using the nanorefrigerant at 0.1 wt.%. Peng et al. [19] investigated the effect of mass fraction on the pressure drop of a boiling R113/CuO nanorefrigerant in a horizontal tube. They concluded that the dispersion of nanoparticles in pure R113 refrigerant increases the drop in pressure. The maximum pressure drop improvement was 20.8%. With a 0.5% mass fraction of CuO nanoparticles distributed in polyester oil, Kedzierski and Gong [20] observed a 275% increase in heat transfer with the base refrigerant R134a. Sun and Yang [8] have investigated nanorefrigerants such as R141b/Cu, R141b/Al_2O_3 and R141b/CuO to find out the effects of material type and quality of vapor on the flow of boiling heat transfer in horizontal tubes with the use of computer-aided tests. The R141b/Cu nanorefrigerant has the highest heat transfer coefficient for the same mass fraction, and R141b/CuO provides the lowest coefficient of heat transfer among the considered nanorefrigerants.

Improvements in heat transfer have been seen in recent studies by the use of Al_2O_3 as nanoparticles in refrigerants, as well as in the reduction of power consumption. Because the heat transfer enhancement reduces the amount of energy required by the compressor to run the working fluid, the system runs more efficiently. Bi et al. [21]examined the R134a/Al2O3 nanorefrigerant in a refrigerator and discovered that a 0.06 wt. percent blend saved 23.24% of energy and increased COP by 18.30 percent. Sabareesh et al. [22] studied how R12/TiO_2/mineral oil could improve a vapor compression cooling system's COP. Based on their findings, compression work decreased by 11% as COP increases in the vapor compression cooling system when the nanorefrigerant is used instead of the R12/MO mixture. The use of nanorefrigerants in domestic refrigerators has been studied by Javadi and Saidur [23] to reduce energy consumption and greenhouse gas emissions. The nanorefrigerants TiO_2-mineral oil-R134a and Al_2O_3-mineral oil-R134a were utilized in mass fractions of 0.06 percent and 0.1 percent, respectively. The nanorefrigerant containing 0.1% TiO_2 nanoparticles showed the highest energy savings. Wang et al. [24] conducted one of the first experimental studies using nanorefrigerant, demonstrating that using TiO_2 nanoparticles in an R134a-based system significantly improves the cooling speed and COP of a domestic refrigerator. Using TiO_2 nanoparticles, Li et al. [25] reported a major increase in the heat transfer coefficient of R11 refrigerant.

In a separate study, Aktas et al. [5] focused on five distinct nanorefrigerants, Al_2O_3 nanoparticles with pure refrigerants; R430a, R436a, R12, R600a, and R134a. The results showed that COP is improved by adding nanoparticles to the pure refrigerants, and the highest increment of 43.93% of COP was obtained by utilizing the R600a/Al_2O_3 mixture. The relationship between thermal power and increased COP performance in some cooling systems was studied by Mahbubul et al. [26]. At the same temperature, the conductivity, dynamic viscosity, and density of the Al_2O_3/R-134a nanorefrigerant rose by 28.58%, 13.68%, and 11%, respectively, when compared to the base refrigerant (R-134a). A nanolubricant of the 40 nm ZnO nanoparticles with PAG oil was prepared by Kumar et al. [27]. The mixture was prepared for 10 h by the magnetic stirrer, then the ultrasonic homogenizer

vibrates the mixture for 15 h to prevent the particles from being clustered. The mixture was then used with R152a refrigerant to develop a nanorefrigerant that decreases the consumption of energy with 0.5% of volume concentration. Kumar et al. [28]evaluated the performance of VCRS with ZrO_2 nanoparticles with R134a and R152a to compare the impact of refrigerant type. ZrO_2 nanoparticles (20 nm) were utilized at 0.01 to 0.06 percent volume concentration. The compressor work for ZrO_2/R152a nanorefrigerant was lower than R152a but higher than R134a. Coumaressin et al. [29] studied the effects of aluminum oxide, copper oxide, titanium oxide, and zinc oxide nanofluids in a vapor compression refrigeration device utilizing R1234yf. Nanofluids are injected directly into the refrigerant in the liquid line after the pump. Using the TK solver, the nanorefrigerant's thermophysical characteristics were assessed. The comparison curves show that Al_2O_3 nanorefrigerant has much better performance than the other nanorefrigerants at 0.55 concentration. The coefficient of performance of Al_2O_3 nanofluid is 28% greater than that of other nanofluids, while power consumption is reduced by 7%.

Although nanorefrigerants have been researched over time, their use in refrigeration is still up for debate. For example, it is observed there is almost no study on the use of nanoparticles with fourth-generation refrigerants. The goal of this research is to examine how nanoparticles affect the thermodynamic efficiency of a cascaded refrigeration system. An investigation into the coefficient of performance (COP) and compressor performance of a cascaded refrigeration system utilizing four different refrigerants, two HFCs as well as two fourth-generation refrigerants (HFOs), namely, the R12, R134a, R1234yf, and R-1234ze (E), in combination with SiO_2 nanoparticles is the goal of this theoretical investigation. The performance of these four nanorefrigerants in a CVCRC is evaluated by introducing SiO_2 nanoparticles at a mass fraction of 0.05%. To investigate the effects of the refrigeration cycle, parameters such as refrigerant type and nanoparticle mass concentration on COP at various evaporation and condensation temperatures. The utilization of SiO_2 nanoparticles synthesized from agricultural waste from the barley plant, which increases sustainability, is another innovative aspect of this research.

Preparation of SiO_2 nanoparticles

Materials and methods

One of the highlights of the research was to synthesize the nanofluid using a sustainable means. Nanosilica was synthesized from the agricultural waste of the barley plant. Barley grass straw (BGS) was collected from levent farm, also hydrochloric acid and sodium hydroxide were prepared for their various molarities, other materials used include furnace, miller equipment, UV reflux bottles, and beakers.

Experimental preparation

The waste straw made from barley was gathered and properly cleansed with distilled water. The barley waste was dried and washed with distilled water, to remove soil particles attached to the straws [30]. After which they were allowed to dry for 24 h at 100 °C in the oven. The dried straw was powdered with the help of a miller and 50 g of the powder was used for preparation. To prepare the nano-enhanced refrigerant fluid, barley grass straw was refluxed in 250 ml of 2 M HCl for 6 h, then heated in a 700 °C furnace for 5 h, the process is the same as described in [31]. The stabilization of the nanoparticle was done by dispersion in deionized water, after which ultra-sonication was carried out to prevent agglomeration and to ensure a pH value of 7.

System description

The CVCRC is divided into two cycles: HTL and LTL. Both cycles have a compressor, condenser, expansion valve, and evaporator, and they are connected by a heat exchanger, which serves as the evaporator in the HTL and the condenser in the LTL at the same time, as shown in Fig. 2. In this study, CO_2 is employed as the working fluid in the LTL loop, whereas one of the four nanorefrigerants is used in the HTL loop. Table 1 summarizes the thermodynamic, environmental, and safety properties of the refrigerants used in this analysis, as obtained from the literature. [33–38]

A schematic of a typical cascaded refrigeration system is given in Fig. 1 and a representative T-S diagram for the CVCRC is presented in Fig. 2. The refrigerant is saturated vapor when it goes into the compressors (points 1 and 5) and saturated liquid when it enters the expansion valves (points 3 and 7). The LTL condenser and the HTL evaporator serve as heat exchangers within the CVCRC. The refrigerant in the HTL cycle evaporates in this heat exchanger, whereas the refrigerant in the LTL cycle condenses into saturated liquid.

The four processes that make up the vapor-compression refrigeration cycle are as follows:

- (1–2), (5–6) isentropically compression of refrigerant in the compressor.
- (2–3), (6–7) constant-pressure condensation,
- (3–4), (7–8) in the expansion valve, adiabatic expansion occurs.
- (4–1), (8–5) constant-pressure evaporation.

Table 1 The thermodynamic, environmental, and safety properties of the refrigerants used

	R125	R134a	R1234yf	R-1234ze (E)	R-744
Chemical formula	C_2HF_5	$C_2H_2F_4$	$C_3H_2F_4$	$C_3H_2F_4$	CO_2
Critical Temperature (°C)	66.02	101.06	94.7	109.36	30.98
Critical Pressure (kPa)	3617.7	4059.28	3382.2	3634.9	7377.3
Critical density (kg/m^3)	573.58	511.899	475.55	489.238	467.6
Boiling point (°C)	−48.09	−26.07	−29.45	−18.97	−78.46
Molecular weight (kg/mol)	120.02	102.032	114.042	114.0416	44.009
GWP*	3170	1300	1	6	1
ODP	0	0	0	0	0
ASHRAE safety group	A1	A1	A2L	A2L	A1
Atmospheric lifetime (years)	29	14	0.030116	NA	200

*Global warming potential with a period of 100 years (CO_2 relative to GWP = 1)

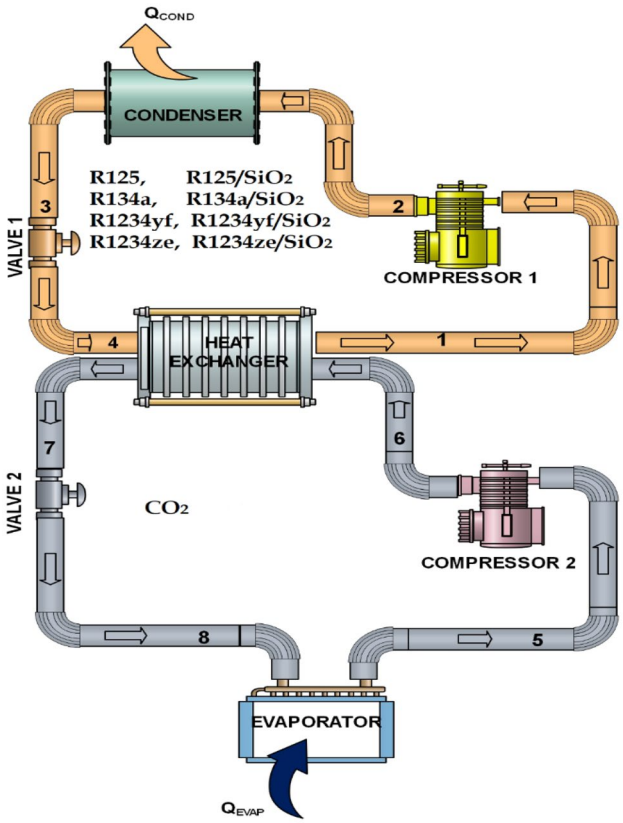

Fig. 1 Schematic of typical cascaded refrigeration system

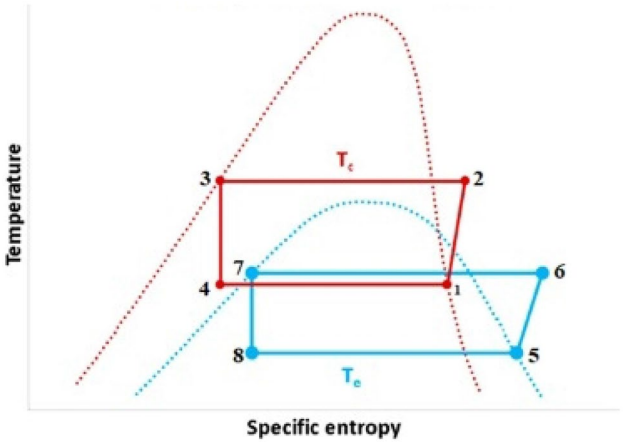

Fig. 2 T-S diagram of a typical cascaded refrigeration system

Theoretical modeling

The mass, energy and entropy balance equations are used to determine the CVCRC's thermodynamic performance, and Table 2 contains the input data used for system analysis. The thermodynamic analysis considers the following assumptions:

- The CVCRC works under steady-state conditions.
- Potential and kinetic energies are insignificant.
- The refrigerant valves are isenthalpic.
- In the CVCRC pipeline, the pressure drops are ignored.
- The nanoparticle distribution in the refrigerant flow is uniform.
- The nanoparticles are not deposited on the solid walls.

For each component of the CVCRC, the mass balance equation is expressed as follows:

$$\sum \dot{m}_{\text{in}} = \sum \dot{m}_{\text{out}} \tag{1}$$

The general energy balance equation for CVCRC is:

$$\sum \dot{m}_{\text{in}} h_{\text{in}} + \sum \dot{Q}_{\text{in}} + \sum \dot{W}_{\text{in}} = \sum \dot{m}_{\text{out}} h_{\text{out}} + \sum \dot{Q}_{\text{out}} + \sum \dot{W}_{\text{out}} \tag{2}$$

Work, specific enthalpy, and heat transfer rates are represented by W, h, and Q, respectively.

Table 2 Input data

	Low-temperature loop (LTL)	High-temperature loop (HTL)
Refrigerant	CO_2	R125, R134, R1234yf, R-1234ze (E) & R125-SiO_2, R134- SiO_2, R1234yf- SiO_2, R-1234ze (E)- SiO_2
Temperature of the evaporator (°C)	−50	–
Temperature of the condenser (°C)	–	–
Temperature of the evaporator (°C)	–	–
Temperature of the condenser (°C)	45	–
Isentropic efficiency of the compressor (%)	80	80
Heat exchanger effectiveness	90	

Table 3 Energy balance

Components	Energy balance
Evaporator	$\dot{m}_8 h_8 + \dot{Q}_{ev} = \dot{m}_5 h_5$
Compressor I	$\dot{m}_1 h_1 + \dot{W}_{comp1} = \dot{m}_2 h_2$
Compressor II	$\dot{m}_5 h_5 + \dot{W}_{comp2} = \dot{m}_6 h_6$
Condenser	$\dot{m}_3 h_3 + \dot{Q}_c = \dot{m}_2 h_2$
Expansion valve I	$\dot{m}_3 h_3 = \dot{m}_4 h_4$
Expansion valve II	$\dot{m}_7 h_7 = \dot{m}_8 h_8$
Heat exchanger	$\dot{m}_4 h_4 + \dot{m}_6 h_6 = \dot{m}_1 h_1 + \dot{m}_7 h_7$

Table 3 represents the energy balance equations for the CVCRC components.

The CVCRC's overall coefficient of performance for cooling is:

$$\mathrm{COP}_{\mathrm{overall}} = \frac{\dot{Q}_{ev}}{\dot{W}_{comp1} + \dot{W}_{comp2}} \tag{3}$$

The density of a nanorefrigerant (NR) is estimated from the density of nanoparticles (NP) and the density of the base fluid (PR) and the mixture ratio using the equation proposed by Xuan and Roetzel [39], it should be noted, however, that the original equation is modified in this work by substituting mass fraction (ω) for volume fraction.

$$\rho_{NR} = \omega\rho_{NP} + (1-\omega)\rho_{PR} \tag{4}$$

Validation

We considered testing for the accuracy and validity of the results by making a comparison between our results and that of the Hussin et al. [40] experimental study as shown in table. Table 4 shows COP for the pure refrigerant R134a and R134a/SiO_2 nanorefrigerant. It can be observed that the COP results from our theoretical analysis and that of Hussin et al. [40] shows same trend; a raise in the COP with the addition of SiO_2 nanoparticles. In the study performed by Hussin et al. [40], a percentage increase of 23.45% in COP value was recorded with the addition of SiO_2, while a percentage increase of 10.11% was recorded in this study. The large deviation is due to the difference in system parameters used in both studies. Also, for this study, only the COP of HTL loop of the cascade system was considered in this validation.

Table 4 Validation of the study

Density of Nanoparticle: Hussin et al. [40]: 2200 kg/m^3, This study:2400 kg/m^3
Mass concentration: Hussin et al. [40]: 0.5%, This study:0.5%

		COP		COP
Pure R134a	Hussin et al. [40]	3.24	This study	2.461
R134a + SiO_2	Hussin et al. [40]	4.00	This study	2.71

Results and discussion

In this study, the thermodynamic performance of a CVCRC using NR is investigated. The nanosilica was synthesized from the agricultural waste of the barley plant. The density of an NR can be used as a metric to measure the enthalpy of a working fluid because there are no charts or correlations to establish the characteristics of NRs. The EES database may be used to calculate nanorefrigerant enthalpies that correspond to the density, temperature, and pressure of pure refrigerants at any point in time. The density of SiO_2 was experimentally determined to be 2400 kg/m^3. It is worth noting that enthalpy of state point 3 on the T-S diagram is calculated as follows; firstly, for this study the condensation temperature (T_{PR3}) and corresponding pressure (P_{PR3}) are set to 45 °C and 1154 kPa, respectively. The density at point 3 of the various pure refrigerants used in this study (R125, R134a, R1234yf, and R-1234ze (E)) are referred to from EES. Nanorefrigerant density (ρ_{NR}) is calculated using Eq. (4). Based on the density of the NR, the enthalpy at

liquid saturation is determined using pure refrigerant data. The latter enthalpy as determined from EES is used to be the one for point 3. Similarly, entropy for point 3 is determined using the EES database. The enthalpy value of NR, determined in this way, is slightly below that of the pure refrigerant used as the base fluid for the NR.

For state point 1, the temperature (T_{PR1}) and saturation pressure (P_{PR1}) are set to − 14 °C and 183.7 kPa, respectively. Enthalpy and entropy of NR at state point 1 are determined in a similar way to that of state point 3. Enthalpy of NR at point 1 is found to be slightly higher than that of pure refrigerant.

The properties of refrigerants at points 1 and 3 are summarized in Table 5.

Using parameters from points 1 and 3 of the refrigeration cycle, such as pressure and entropy, the enthalpy of points 2 and 4 can be calculated. h_4 at the evaporator's inlet must equal h_3 due to adiabatic expansion in the expansion valve. EES calculates h_1 using s_1 and saturation pressure at point 3. Furthermore, if the compressors' isentropic efficiency is equal to 1 and the refrigeration cycle is ideal, s_1 and s_2 at the compressor's outlet must be equal. The compressor's isentropic efficiency is assumed to be 0.80 in this study.

Results from nanoparticle characterization

To obtain the XRF patterns of SiO_2 nanoparticles, the samples are measured with an X-ray diffractometer (Bruker D8 Advance model). Following that substantial peaks were noticed and recorded over the range of 400–4000 cm^{-1} utilizing (IR Prestigue–21 Shimadzu, Japan) to explore the characteristics of nanoparticles. This analysis is critical for identifying the functional groups in nanoparticles. It was important to perform EDX analysis to determine the constituent elements. In the SEM analysis, the EDX generates X-rays based on the principle of electrons focused primarily on the specimen. As a result, it is possible to provide a complete depiction of the constituent elements [32].

Figure 3 shows the FTIR spectra of produced silica nanoparticles after calcination at 700 °C. The domineer peaks point to the occurrence of silica. Vibrations related to the stretching of silicon bonds (Si–O–Si) for NS synthesized from BGS cause the peak at 1080 cm^{-1}. In addition, the vibrations have a low critical stretching peak. In the FTIR, NS synthesized from BGS has a transmission spectrum of 400–4000 cm^{-1}. A peak at 2250 cm^{-1} was also linked to an aromatic methyl group's C=H bond stretching. The peak at 800 cm^{-1} revealed siloxane linkages (Si–O–Si) framing silica from silicon, demonstrating that the findings of this study are consistent with previous findings. Figure 3 also shows SEM images in which no aggregation and less agglomeration was observed in the structures. At around 2.0 keV, a significant silicon peak was seen, indicating that 88.6% of silicon was synthesized.

Some basic properties of the synthesized barley grass nanosilica (SiO_2) are tabulated in Table 6.

Results of the sensitivity analysis

For all refrigerant couplings at constant evaporator temperature (T_{ev} = − 50 °C), Fig. 4 examines the effect of condenser temperature on overall CVCRC COP. As the condenser temperature rises from 25 to 50 °C, the total COP decreases in all situations. Among the refrigerant couples studied, the R1234ze/SiO_2(NR)-CO_2 refrigerant pair has the highest overall COP value, while the R125-CO_2 refrigerant couple has the lowest overall COP value.

The effect of the condenser temperature on the CVCRC evaporator's heat transfer rate is seen in Fig. 5. The figure depicts a declination trend, in which the heat of evaporation of the refrigerants increases as the temperature increases. The evaporator heat rate is increased by lower condenser temperatures. It was also discovered that adding silicon

Table 5 Properties of nanorefrigerants at points 1 and 3

State point	T_{PR}(°C)	ρ_{PR}(kg/m^3)	h_{PR}(kJ/kg)	ω	ρ_{SiO_2}(kg/m^3)	ρ_{NR}(kg/m^3)	T_{NR}	h_{NR}(kJ/kg)
R125/SiO$_2$								
1	− 15	25.54	325.67	0.0005	2400	26.73	− 13.7	326.34
3	45	1048	262.66	0.0005	2400	1049	44.93	262.55
R134a/SiO$_2$								
1	− 15	8.293	241.48	0.0005	2400	9.489	− 11.51	243.60
3	45	1125	115.80	0.0005	2400	1126	44.85	115.58
R1234yf/SiO$_2$								
1	− 15	10.5	353.39	0.0005	2400	11.69	− 12.04	355.35
3	45	1012	261.14	0.0005	2400	1013	44.82	260.88
R-1234ze (E)/SiO$_2$								
1	− 15	6.831	373.64	0.0005	2400	8.028	− 10.84	376.57
3	45	1092	263.02	0.0005	2400	1093	44.84	262.78

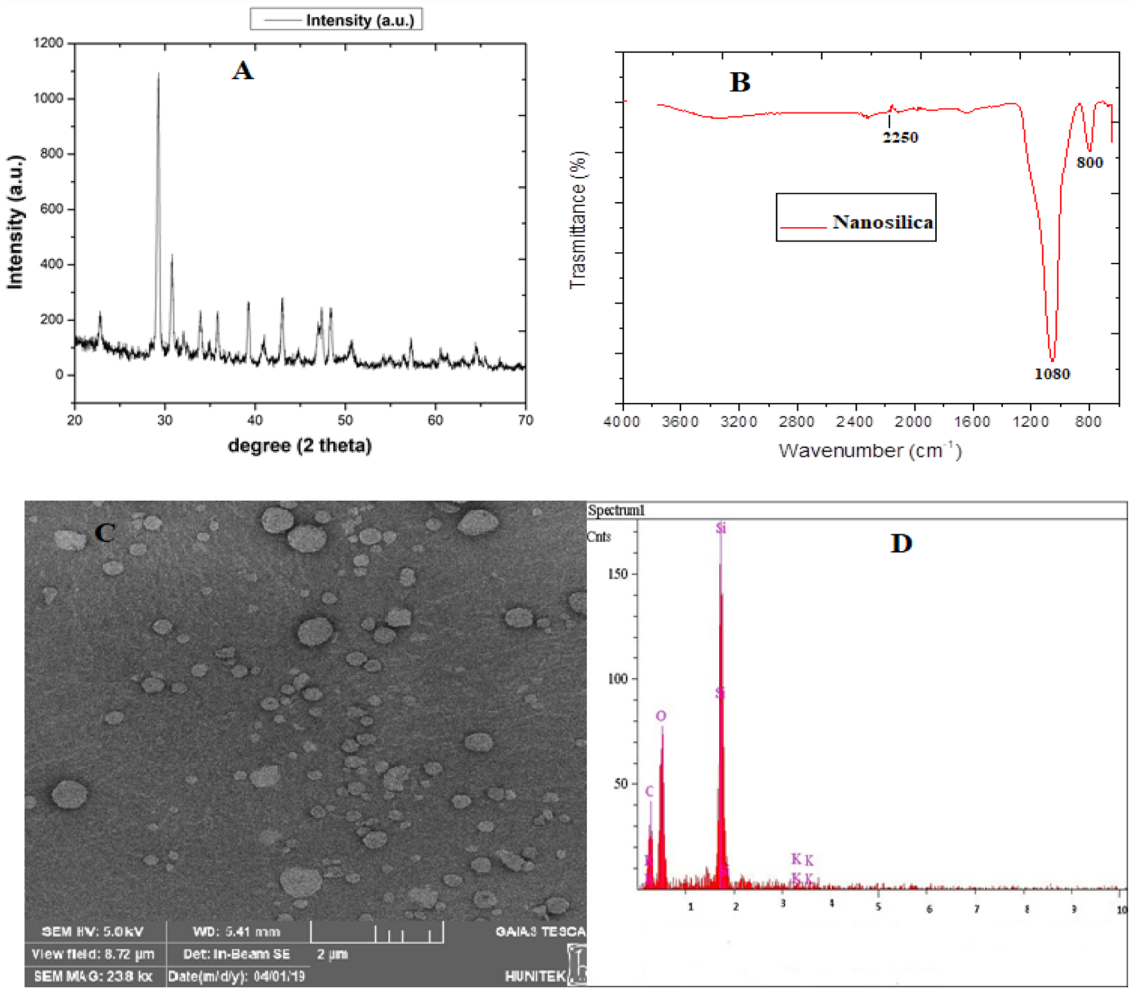

Fig. 3 **A** Xrd Images of Nanosilica, **B** Ftir of Nanosilica, **C** Sem Images of Nanoparticles, **D** Edx images of nanoparticles

Table 6 Synthesized barley grass nanosilica (SiO_2) properties

Property	
Density (kg/m^3)	2400
Thermal conductivity (W/m.K)	1.380
Specific heat capacity (J/kg.K)	968.9
Particle size (nm)	100

oxide (SiO_2) nanoparticles to the base refrigerants enhanced the evaporator's heat transfer rate.

The influence of evaporator temperature on the overall COP of the CVCRC is illustrated in Fig. 6, while the condenser temperature remains constant at 45 °C. The COP of the CVCRC increases as the evaporator temperature rises from − 55 °C to − 40 °C for all refrigerant pairs. The R1234ze/SiO_2-CO_2 refrigerant pair has the highest COP, with a 23.95% increase when the evaporator temperature is adjusted from − 55 °C to − 40 °C while the condenser

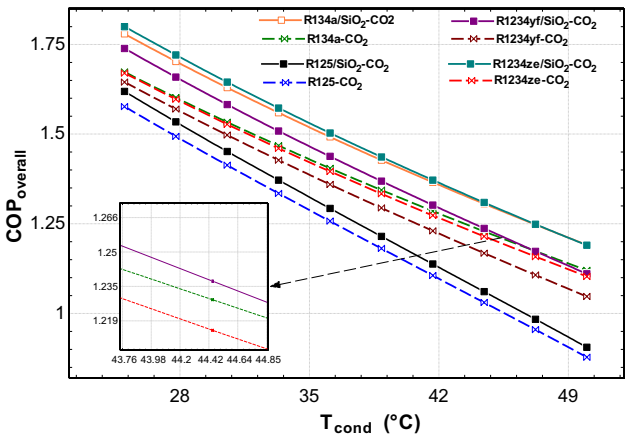

Fig. 4 Effect of condenser temperature on overall COP at $T_{evap} = -50$ °C

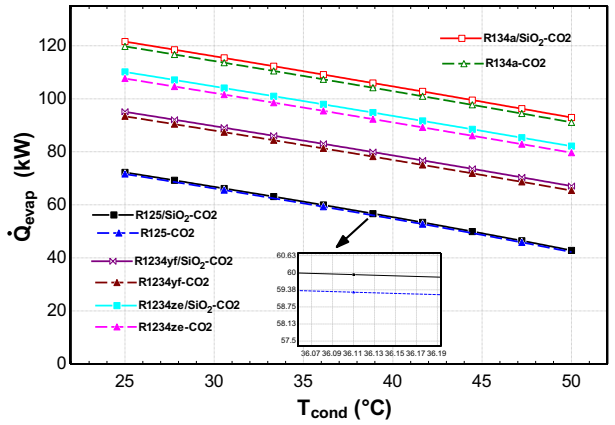

Fig. 5 Effect of Condenser Temperature on Evaporator load at $T_{evap} = -50$ °C

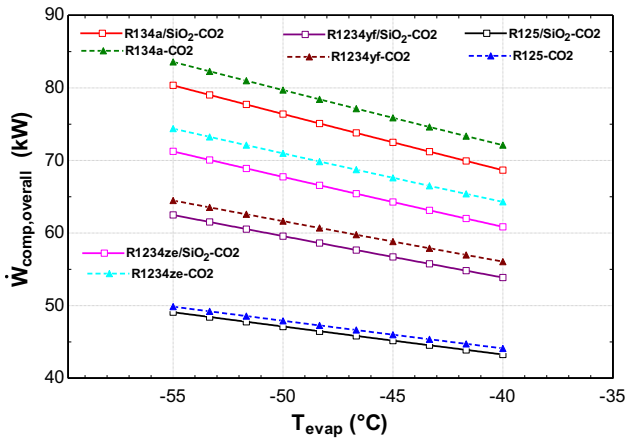

Fig. 7 Effect of Evaporator temperature on Overall compressor work ($T_{cond} = 45$ °C)

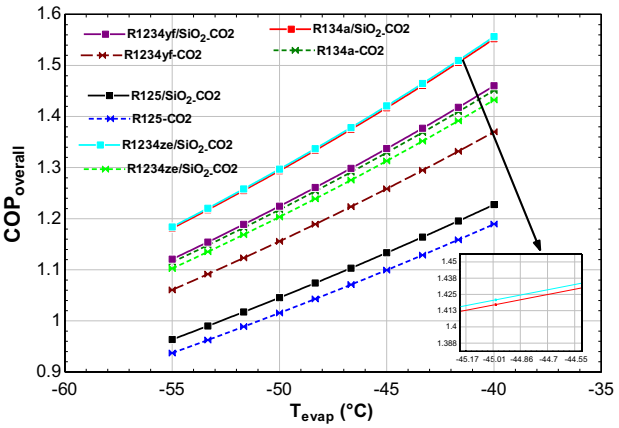

Fig. 6 Effects of Evaporator temperature on Overall COP at $T_{cond} = 45$ °C

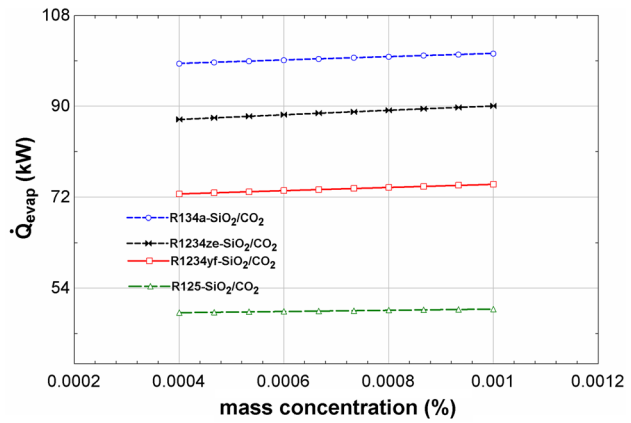

Fig. 8 Effect of mass concentration of nanoparticle on the refrigeration effect

temperature is kept at 45 °C. Krishnan et al. [41] reported a similar trend and observations in a similar investigation.

At a constant condenser temperature of 45 °C, Fig. 7 shows the effect of evaporator temperature on compressor work. As predicted, the compressor consumes less energy at higher evaporator temperatures while the condenser temperature remains constant. It was observed that compressor work decreased by adding silicon oxide (SiO_2) nanoparticles to the base refrigerants. A rise in COP was caused by an increase in Q_e and a decrease in W_{comp}, as per Eq. (4). This means that less energy is consumed for the same refrigeration capacity. Among the refrigerants investigated, R134a-CO_2 had the highest compressor work while R125/SiO_2-CO_2 had the lowest compressor work in all conditions at a constant condenser temperature.

Figure 8 depicts the effect of increasing the mass concentration of the SiO_2 nanoparticles on the refrigeration effect of the CVCRC. Increasing the mass concentration from 0.04% to 0.1% leads to an increase in the refrigeration effect. This is because more nanoparticles per unit mass of refrigerant improve the heat transfer coefficient and thus the cooling effect.

Figure 9 shows the influence of nanoparticle mass concentration on overall compressor work and COP of the CVCRC employing four different nanorefrigerants. For the four nanorefrigerants, the work of the compressor decreases as the mass concentration increases. The mobility of the nanoparticle within the nanorefrigerant contributes to the pressure of the nanorefrigerant, which requires the compressor to do less work to achieve the required condenser pressure. As a result, the quantity of work required by the compressor is greatly reduced. The COP increases as mass concentration rises. Because there are more nanoparticles per unit of refrigerant, the heat transfer coefficient and COP are greatly enhanced [42]. Odunfa and Oseni [42] likewise noted and documented this facts and pattern.

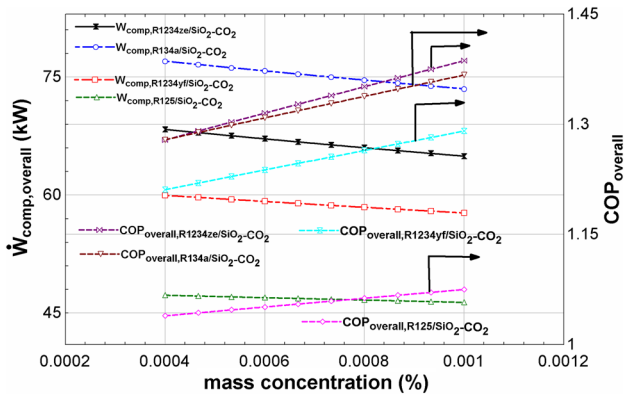

Fig. 9 Effect of mass concentration of the nanoparticles on the overall compressor work and COP

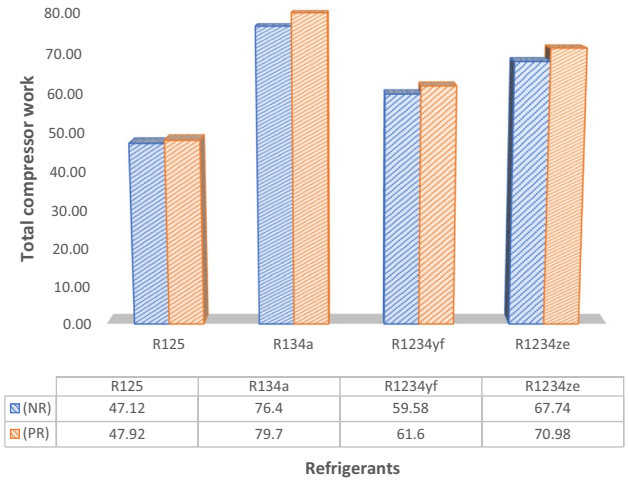

	R125	R134a	R1234yf	R1234ze
(NR)	47.12	76.4	59.58	67.74
(PR)	47.92	79.7	61.6	70.98

Fig. 11 Comparison of total compressor work for different refrigerant pairs

The CVCRC COP was determined to be 1.045, 1.015, 1.294, 1.218, 1.224, 1.156, 1.297, and 1.203 for R125/SiO2-CO2, R125-CO2, R134a/SiO2-CO2, R134a-CO2, R1234yf/SiO2-CO2, R1234yf-CO2, R1234ze/SiO2-CO2, and R1234ze-CO2 refrigerant. The results demonstrate that the best performing HFC refrigerant (with and without nanoparticles) is R134a, while the best performing fourth generation refrigerant (with and without nanoparticles) is R1234ze; exhibiting a very close margin to the best performing HFC refrigerant (Fig. 10).

In Fig. 11, it was observed that compressor work decreases by adding silicon oxide (SiO_2) nanoparticles to the base refrigerants. This occurs because the nanoparticles enhance heat transfer performances and decrease energy consumption in the compressor. From Fig. 8, it is seen that the usage of R125 nanorefrigerant in high temperature loop of the CVCRC system decreases compressor work by 1.66%, 4.1% when R134a nanorefrigerant is used, 3.27% when

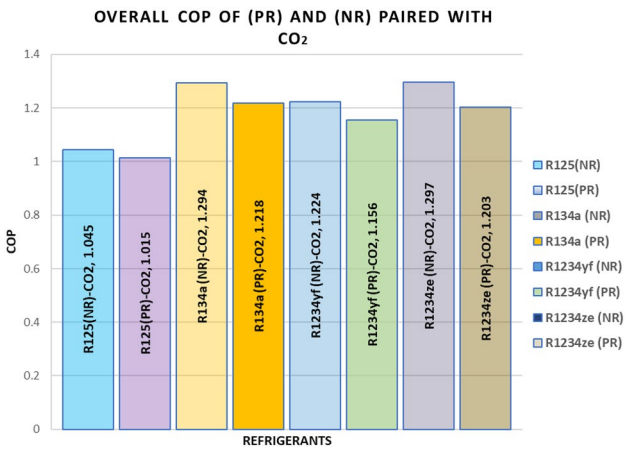

Fig. 10 COP comparison of the CVCRC for all cases of refrigerant couples ($T_{evap} = -50$ °C, $T_{cond} = 40$ °C)

R1234yf nanorefrigerant is used and 4.56% when R1234ze nanorefrigerant is used.

Conclusion

Comparing the effects of adding SiO_2 nanoparticles to different refrigerants was carried out in this study. The nanosilica was synthesized from the agricultural waste of the barley plant. One major aim of the research was to synthesize the nanofluid using a sustainable means. A numerical model is adopted for the thermodynamic analysis of the system and the results were based on the coefficient of performance (COP), compressor work, mass concentration, evaporation heat, and condenser heat. It was difficult to determine the enthalpy of the nanorefrigerant due to the fact there is a scarcity of correlation or experimental data in this field. As a result, calculations for the enthalpy of nanorefrigerants in the refrigerant cycle were made using a density prediction method for nanorefrigerants. Findings from the study indicates that the thermal properties of refrigerant fluids are improved by adding nanoparticles, which increases the refrigeration system's performance.

In the cycles using nanorefrigerants, the COP was shown to be greater. R1234ze/SiO_2-CO_2 refrigerant couple had the highest COP, followed by the R134a/SiO_2-CO_2 under all of the conditions investigated in the study. Increasing the evaporator temperature from − 55 to − 40 °C led to an increase in the COP for all refrigerant pairs.

The results indicate that adding 0.05% mass concentration of SiO_2 nanoparticles to base refrigerants improves the overall performance of the CVCRC over pure-base refrigerants.

Addition of SiO_2 nanoparticles resulted to a reduction in compressor work. Despite the fact that R125 had the

lowest compressor work. In its place, R1234ze, the refrigerant with the second-lowest compressor work can be used, with the addition of SiO_2 compressor work is reduced to 59.58kW from 61.6 kW. It also has a GWP of 6, and may be successfully used in newly designed systems instead of R134a. The use of nanoparticles therefore, improves the refrigeration cycle's performance by improving heat transfer in heat exchangers and lowering the compressor's power consumption.

Moreover, the nanoparticle is likely dispersed in the liquid rather than the gas phase. Therefore, this work brings together a number of approximations and gives a useful tool for scholars to use in their work. Analytical models for predicting physical properties have gotten very little attention. More work will be required to make this study popular. Additionally, more investigation is still needed to determine how other nanoparticle properties affect a vapor compression refrigeration system.

References

1. Mahbubul, I.M., Saidur, R., Amalina, M.A.: Influence of particle concentration and temperature on thermal conductivity and viscosity of Al2O3/R141b nanorefrigerant. Int. Commun. Heat Mass Transf. **43**, 100–104 (2013)
2. Adebayo, V., Abid, M., Adedeji, M., Dagbasi, M., Bamisile, O.: Comparative thermodynamic performance analysis of a cascade refrigeration system with new refrigerants paired with CO2. Appl. Therm. Eng. (2020). https://doi.org/10.1016/j.applthermaleng.2020.116286
3. Kumar, V.: Comparative analysis of cascade refrigeration system based on energy and exergy using different refrigerant Pairs. J. Therm. Eng. **6**(1), 106–116 (2020)
4. Sanukrishna, S.S., Vishnu, A.S.: Nanorefrigerants for energy efficient refrigeration systems. J. Mech. Sci. Technol. **31**(8), 3993–4001 (2017)
5. Aktas, M., Dalkilic, A.S., Celen, A., Cebi, A., Mahian, O., Wongwises, S.: A theoretical comparative study on nanorefrigerant performance in a single-stage vapor-compression refrigeration cycle. Adv. Mech. Eng. **7**(1), 138725 (2015)
6. Celen, A., Çebi, A., Aktas, M., Mahian, O., Dalkilic, A.S., Wongwises, S.: A review of nanorefrigerants: flow characteristics and applications. Int. J. Refrig. **44**, 125–140 (2014)
7. Fang, X., Wang, R., Chen, W., Zhang, H., Ma, C.: A review of flow boiling heat transfer of nanofluids. Appl. Therm. Eng. **91**, 1003–1017 (2015)
8. Sun, B., Yang, D.: Flow boiling heat transfer characteristics of nano-refrigerants in a horizontal tube. Int. J. Refrig. **38**, 206–214 (2014)
9. Alawi, O.A., Sidik, N.A.C., Kherbeet, A.S.: Nanorefrigerant effects in heat transfer performance and energy consumption reduction: a review. Int. Commun. Heat Mass Transf. **69**, 76–83 (2015)
10. Gupta, S., Karanam, N.K., Konijeti, R., Dasore, A.: Thermodynamic analysis and effects of replacing HFC by fourth-generation refrigerants in VCR systems. Int. J. Air-Conditioning Refrig. **26**(02), 1850013 (2018)
11. Perkins, J.: Apparatus for producing ice and cooling fluids. Br. Pat., no. 6662, 1834
12. Nagengast, B.A.: A history of refrigerants. CFCs Time Transit. (1989)
13. de Chazournes, L.B.: Kyoto protocol to the united nations framework convention on climate change. UN's Audiov. Libr. Int. Law (http//untreaty. un. org/cod/avl/ha/kpccc/kpccc. html). (1998)
14. Montzka, S.A., Hall, B.D., Elkins, J.W.: Accelerated increases observed for hydrochlorofluorocarbons since 2004 in the global atmosphere. Geophys. Res. Lett. (2009). https://doi.org/10.1029/2008GL036475
15. Fluorochemicals, D.: DuPont fluorochemicals develops next generation refrigerants–new sustainable alternatives would offer practical solutions. Press Release. Wilmington, DE, USA (09.02. 06). (2006)
16. Kasaeian, A., Hosseini, S.M., Sheikhpour, M., Mahian, O., Yan, W.-M., Wongwises, S.: Applications of eco-friendly refrigerants and nanorefrigerants: a review. Renew. Sustain. Energy Rev. **96**, 91–99 (2018)
17. Subramani, N., Prakash, M.J.: Experimental studies on a vapour compression system using nanorefrigerants. Int. J. Eng. Sci. Technol. **3**(9), 95–102 (2011)
18. Jwo, C.S., Jeng, L.Y., Teng, T.P., Chang, H.: Effects of nanolubricant on performance of hydrocarbon refrigerant system. J. Vac. Sci. Technol. B Microelectron. Nanom. Struct. Process. Meas. Phenom. **27**(3), 1473–1477 (2009)
19. Peng, H., Ding, G., Jiang, W., Hu, H., Gao, Y.: Measurement and correlation of frictional pressure drop of refrigerant-based nanofluid flow boiling inside a horizontal smooth tube. Int. J. Refrig. **32**(7), 1756–1764 (2009)
20. Kedzierski, M.A.: Effect of CuO nanoparticle concentration on R134a/lubricant pool-boiling heat transfer. J. Heat Transf. (2009). https://doi.org/10.1115/1.3072926
21. Bi, S., Shi, L., Zhang, L.: Application of nanoparticles in domestic refrigerators. Appl. Therm. Eng. **28**(14–15), 1834–1843 (2008)
22. Sabareesh, R.K., Gobinath, N., Sajith, V., Das, S., Sobhan, C.B.: Application of TiO2 nanoparticles as a lubricant-additive for vapor compression refrigeration systems–an experimental investigation. Int. J. Refrig. **35**(7), 1989–1996 (2012)
23. Javadi, F.S., Saidur, R.: Energetic, economic and environmental impacts of using nanorefrigerant in domestic refrigerators in Malaysia. Energy Convers. Manag. **73**, 335–339 (2013)
24. Wang, R. X., Hao, B., Xie, G.Z., Li, H.Q.: A refrigerating system using HFC134a and mineral lubricant appended with n-TiO2 (R) as working fluids. In: Proceedings of the 4th International Symposium on HAVC, Tsinghua University Press, Beijing, China, 2003, pp. 888–892
25. Li, P., Wu, X., Li, H., Wang, W.: Investigation of Pool boiling heat transfer of R11 with TiO~ 2 nano-particles. J. Eng. Thermophys. **29**(1), 124 (2008)
26. Mahbubul, I.M., Saadah, A., Saidur, R., Khairul, M.A., Kamyar, A.: Thermal performance analysis of Al2O3/R-134a nanorefrigerant. Int. J. Heat Mass Transf. **85**, 1034–1040 (2015)
27. Kumar, D.S., Elansezhian, R.: ZnO nanorefrigerant in R152a refrigeration system for energy conservation and green environment. Front. Mech. Eng. **9**(1), 75–80 (2014)
28. Kumar, V.P.S., Baskaran, A., Subaramanian, K.M.: A performance study of vapour compression refrigeration system using ZrO2 nano particle with R134a and R152a". Int. J. Sci. Res. Publ. **6**, 410–421 (2016)
29. Coumaressin, N.A.T., Palaniradja, K.: Experimental Analysis of a Refrigeration system using Al2O3/CuO/TiO2/ZnO-R1234yf Nanofluids as refrigerant. Int. J. Res. Eng. Appl. Manag. **4**(08), 69–75 (2018)
30. Bhattacharya, M., Mandal, M.K.: Synthesis of rice straw extracted nano-silica-composite membrane for CO2 separation. J. Clean. Prod. **186**, 241–252 (2018)

31. Essien, E.A., Kavaz, D.: Effective and reusable nano-silica synthesized from barley and wheat grass for the removal of nickel from agricultural wastewater. Environ. Sci. Pollut. Res. **26**(25), 25802–25813 (2019)
32. Akhayere, E., Vaseashta, A., Kavaz, D.: Novel magnetic nano silica synthesis using barley husk waste for removing petroleum from polluted water for environmental sustainability. Sustain. **12**(24), 1–16 (2020). https://doi.org/10.3390/su122410646
33. Handbook, A.: ASHRAE handbook–fundamentals. Atlanta, GA. (2009)
34. McLinden, M.J.O., Thol, M., Lemmon, E.W.: Thermodynamic properties of trans-1, 3, 3, 3-tetrafluoropropene [R1234ze (E)]: measurements of density and vapor pressure and a comprehensive equation of state. (2010)
35. Steven Brown, P.E.J.: Methodology for estimating thermodynamic parameters and performance of alternative refrigerants. ASHRAE Trans. **114**: 230 (2008)
36. Steven Brown, P.E.J.: HFOs: new, low global warming potential refrigerants. ASHRAE J. **51**(8), 22 (2009)
37. Di Nicola, C., Di Nicola, G., Pacetti, M., Polonara, F., Santori, G.: P− V− T Behavior of 2, 3, 3, 3-Tetrafluoroprop-1-ene (HFO-1234yf) in the vapor phase from (243 to 373) K. J. Chem. Eng. Data. **55**(9), 3302–3306 (2010)
38. Del Col, D., Torresin, D., Cavallini, A.: Heat transfer and pressure drop during condensation of the low GWP refrigerant R1234yf. Int. J. Refrig. **33**(7), 1307–1318 (2010)
39. Xuan, Y., Roetzel, W.: Conceptions for heat transfer correlation of nanofluids. Int. J. Heat Mass Transf. **43**(19), 3701–3707 (2000)
40. Hussin, M.H.C., Mahadi, M.A.S., Sanuddin, A., Khalil, A.N.M., Rahim, Y.A.: Experimental performance of R134a/SiO2 in refrigeration system for domestic use. J. Adv. Res. Fluid Mech. Therm. Sci. **95**(1), 145–163 (2022)
41. Krishnan, B.P., Vijayan, R., Gokulnath, K.: Performance analysis of a nano refrigerant mixtures in a domestic refrigeration system. Adv. Nat. Appl. Sci. **11**(6), 508–516 (2017)
42. Odunfa, M.K., Oseni, O.D.: Numerical simulation and performance assessment of a nanoparticle enhanced vapour compression refrigeration system. J. Power Energy Eng. **9**(11), 33–49 (2021)